Energy dissipation in silicon nitride microbeam resonators with a 3D-printed polymer layer

Crocetto, Lucia; Manzaneque, Tomás; Ghatkesar, Murali Krishna

DOI
10.1016/j.mne.2025.100300

Publication date
2025

Document Version
Final published version

Published in
Micro and Nano Engineering

MNE 28 (2025) 100300

Contents lists available at ScienceDirect

Micro and Nano Engineering

journal homepage: www.sciencedirect.com/journal/micro-and-nano-engineering

Research paper

Energy dissipation in silicon nitride microbeam resonators with a 3D-printed polymer layer

Lucia Crocetto [a], Tomás Manzaneque [a,1], Murali Krishna Ghatkesar [b,*,1]

[a] Department of Microelectronics, Delft University of Technology, 2628 CD Delft, the Netherlands
[b] Department of Precision and Microsystems Engineering, Delft University of Technology, 2628 CD Delft, the Netherlands

ARTICLE INFO

Keywords:
Microbeams
3D printing
Two-photon polymerization
Mechanical resonators
Damping
Dissipation

ABSTRACT

We present an analysis of the main mechanisms of dissipation of resonant multilayer double-clamped microbeams in the frequency range 200 to 500 kHz. The devices consist of 2 μm thick silicon nitride (E $\approx$ 160 GPa) beams covered with a polymer IP-Dip (E $\approx$ 4 GPa) layer fabricated by two-photon polymerization. A laser-Doppler vibrometer was used to measure the resonant vibrations and energy dissipation of the devices in high vacuum ($<$ 0.05 Pa) at room temperature. The experimental findings were compared with theoretical and finite element method (FEM) results. The quality factor, dominated by the intrinsic dissipation in the IP-Dip layer, has proven to have a strong dependence on polymer thickness. On this basis, a viscous model for intrinsic dissipation in a polymer layer was formulated.

1. Introduction

With the introduction of additive manufacturing techniques, such as two-photon polymerization (TPP), polymers can be directly 3D-structured to be integrated into lithography-fabricated micro-electromechanical systems (MEMS) leading to hybrid manufacturing. In resonant microstructures, TPP-printed polymer on a silicon-based device can be used for various applications ranging from mass and chemical sensing [1,2] to atomic force microscopy [3]. Therefore, an investigation of the dissipation in multilayer microresonators including a polymer layer with viscoelastic properties is needed. Even though energy losses in both silicon-based and TPP-printed polymer microbeams have been thoroughly investigated [4,5], hybrid devices still need simple models to describe their dynamics.

In this paper, we analyzed the dissipation mechanisms of double-clamped microbeams made of silicon nitride (E $\approx$ 160 GPa) and subsequently 3D-printed with IP-Dip, a commercial acrylic-based photopolymer, layered on top (E $\approx$ 4 GPa) [6]. Polymer layers with varying geometry were TPP-printed on SiN_x beams of different lengths to study dissipation in a frequency range from 200 to 500 kHz.

The energy dissipated in a mechanical resonator is expressed by its quality factor, *Q*, derived from a combination of energy loss mechanisms, and given by eq. 1

$$1/Q = 1/Q_{med} + 1/Q_{cl} + 1/Q_{int} + 1/Q_{others} \quad (1)$$

where Q_{med} is due to the resonator-medium interaction, Q_{cl} is due to the acoustic losses at the clamping sites, Q_{int} is due to the internal dissipation within the resonator, in the bulk and on the surface, and Q_{others} denotes other energy losses. In the case of a multilayer beam, each i-th layer composing the device contributes to the internal dissipation by introducing a distinct internal dissipation source. Therefore, in our simplified model, we assume that the overall Q_{int}^{-1} can be obtained as the sum of the inverted Q-factors of each layer i, $Q_{int,i}^{-1}$.

In this work, we investigated the contribution of different material layers to the energy dissipation of doubly-clamped SiN_x microbeam resonators. When operated in air, medium interaction dissipation is dominant in our multilayer resonators. However, this contribution is significantly reduced under high vacuum conditions. Operating in vacuum allowed us to neglect Q_{med} in eq. 1 and study the effect of clamping and intrinsic dissipation. Clamping dissipation is strictly related to the anchor geometry [7], i.e., thickness and length of the SiN_x beam, and anchor width of the polymer layer. Meanwhile, intrinsic dissipation is a material-dependent factor. An initial analysis was carried out to characterize the intrinsic dissipation in SiN_x; then, the impact of added Al-Si (1 %) and IP-Dip layers on the overall dissipation of the beam was analyzed.

* Corresponding author at: Mekelweg 2, 2628 CD Delft, the Netherlands.
E-mail addresses: l.crocetto@tudelft.nl (L. Crocetto), t.manzanequegarcia@tudelft.nl (T. Manzaneque), m.k.ghatkesar@tudelft.nl (M.K. Ghatkesar).
[1] Equal contribution

https://doi.org/10.1016/j.mne.2025.100300
Received 25 May 2025; Accepted 31 May 2025
Available online 5 June 2025

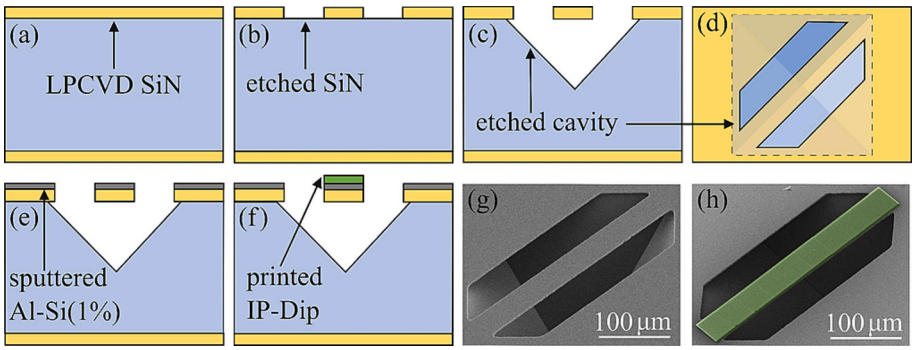

Fig. 1. Fabrication process flow and manufactured device. a Low-stress SiN_x deposition, b SiN_x dry etching, c and d KOH top-side etching, e Al-Si(1 %) sputtering, f TPP of the polymer. Isometric SEM images of 300 μm long, 50 μm wide, 2 μm thick SiN_x beam coated with 30 nm Al-Si(1 %) g before and h after 3D-printing of 4 μm thick IP-Dip layer (green). (For interpretation of the references to colour in this figure legend, the reader is referred to the web version of this article.)

Table 1
Comparison of Simulated and Experimental Frequencies of 2 μm Thick SiN_x Beams of Different Length Before and After Al-Si(1 %) Sputtering.

Length	SiN_x FEM	SiN_x Exp.	SiN_x + Al-Si(1 %) FEM	SiN_x + Al-Si(1 %) Exp.
(μm)	(kHz)	(kHz)	(kHz)	(kHz)
250	614	607 ± 4	613	606 ± 3
300	501	484 ± 3	501	487 ± 1
350	424	406 ± 3	424	407 ± 2
400	367	352 ± 1	367	349 ± 3
450	324	305 ± 2	324	305 ± 3
500	290	271 ± 2	290	271 ± 2

2. Materials and methods

Double-clamped 2 μm thick and 50 μm wide SiN_x beams with a length ranging from 250 to 500 μm were fabricated from low-stress LPCVD on a ⟨100⟩ silicon wafer. Beams were patterned by a single-mask photolithographic process and released by top-side KOH etching. The front-side etch process fully released the microbridges as the beams were rotated 45° from the ⟨110⟩ direction. The reflectivity of the beams was increased by sputtering a 30 nm thick Al-Si(1 %) layer for easy identification of the surface in the subsequent TPP printing. Then, a polymer IP-Dip layer was patterned by TPP on top of each beam including clamping regions. Fig. 1 shows the fabrication flowchart and an SEM image of a fabricated microbeam. Two different polymer structures printed on metal-coated SiN_x beams were investigated: first, a polymer layer of fixed thickness (1 μm) and variable width at the anchors, and second, a layer of variable thickness fully covering the microbeam (43 μm wide).

The stress within the SiN_x layer was obtained by measuring the wafer curvature before and after LPCVD deposition with a Flexus 2320-S thin-film stress measurement instrument. The measurement after deposition was performed after the backside etching of the SiN_x layer. The average stress of the deposited film was derived from Stoney's Eq. [8]. The resonating structures were actuated by placing the chip on an external piezoelectric element in a vacuum chamber. The vibration was monitored at the center of the beam with an MSA-400-PM2-D Laser Doppler vibrometer operated in a frequency range from 0 to 2 MHz. The fundamental mode was measured, and the resonant frequency was determined by performing a Fast Fourier Transform (FFT) and fitting the resulting resonant peak. All measurements were performed at room temperature in high vacuum (< 0.05 Pa). No significant change in Q was observed for pressures below 10 Pa, indicating negligible medium dissipation at the working pressure. The thicknesses of the polymer layers were measured with a white light interferometer, after a 25 nm-thick gold layer was sputtered on the sample to increase its reflectivity.

The error bars shown in the graphs were calculated as the semi-range of the experimental data points. This was determined from two sets of measurements performed on different devices fabricated for each geometry. Uncertainties from instrumental precision were negligible in comparison with the observed spread in the experimental results.

3. Results and discussion

3.1. SiN_x beams

A comparison of FEM simulated and experimental fundamental resonant frequencies is shown in Table 1. The FEM simulations were performed taking into account the measured undercut of 5 μm and the experimentally determined internal stress of 237 MPa in the SiN_x layer. The tensile stress was included in the model by applying an initial stress condition to the SiN_x beam. FEM results exhibit an error within 7 % when compared to the experiments. This can be attributed to manufacturing tolerances, i.e., photolithography with foil mask, and KOH over-etching, influencing beam size and clamping conditions.

Fig. 1(a) shows the values of the experimental Q-factors. The measurements of SiN_x beams (blue bars) revealed a non-monotonic variation of Q with length, contrary to the theoretical prediction of clamping dissipation [7]. This result suggests that clamping losses are not dominant in SiN_x beams and intrinsic dissipation might be the main dissipation source. This is in agreement with other studies on SiN_x resonators, which have proven thermoelastic dissipation to be the main dissipation source [5].

3.2. SiN_x beams with metal layer

FEM simulated and experimental fundamental resonant frequencies after depositing a 30 nm thick Al-Si(1 %) layer are reported in Table 1. The simulations show negligible frequency shifts as a result of the additional metal layer. This is due to the low thickness of the layer, that entails a negligible impact on the overall mass and stiffness of the beam. The variation of the measured fundamental frequency and the Q-factor for beams of different lengths after metal coating are shown in Fig. 1. Although the thin metal layer has been proven to have a negligible effect on the resonant frequency (the frequency shift is of the same order as the error in experimental frequencies of bare SiN_x beams), it shows a considerable impact on Q ($>$ 48 % reduction). Indeed, soft metals are characterized by high internal friction, and this occurs even for extremely thin coatings [9]. In addition, sub-micrometer thick layers exhibit high surface friction loss due to roughness, impurities, and surface adsorbates [7]. It follows that dissipation in metal-coated SiN_x beams is highly influenced by friction in metal.

3.3. SiN_x beams with metal layer and polymer layer

Adding a polymer layer causes a resonant frequency shift inversely

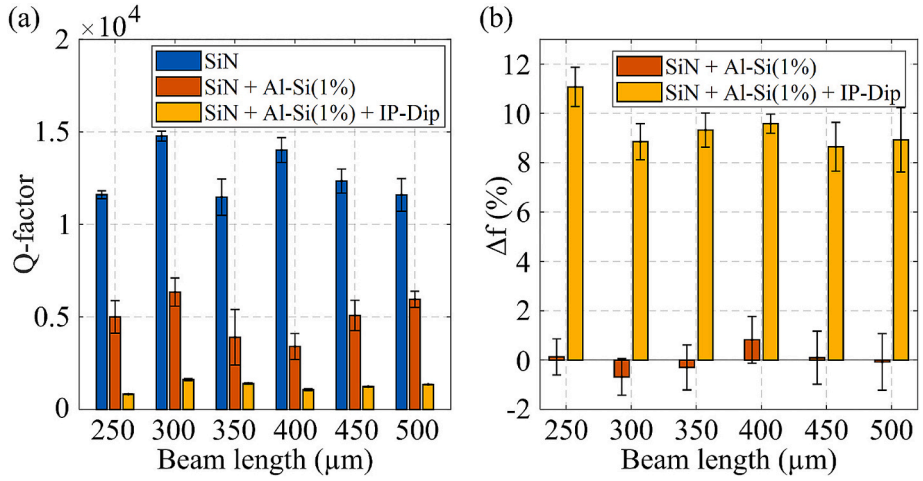

Fig. 2. Experimental Q-factors and resonant frequencies. a Q-factors of 2 μm thick SiN_x beams, Al-Si(1 %) coated 2 μm thick SiN_x beams, and Al-Si(1 %) coated 2 μm thick SiN_x beams with 1 μm thick IP-Dip layer. b Resonant frequency variation due to additional Al-Si(1 %) and IP-Dip layers on 2 μm thick SiN_x beams. Error bars were calculated with the semi-range method by performing two sets of measurements on three devices for each geometry.

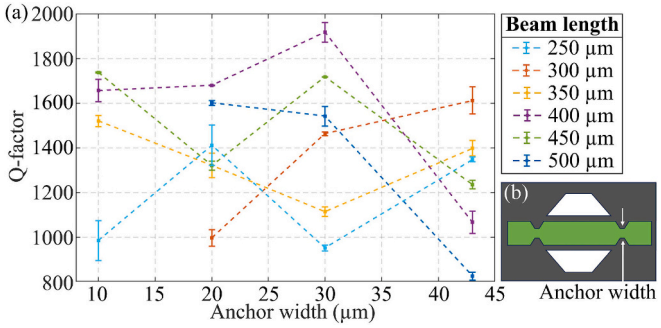

Fig. 3. Experimental study of the polymer clamping dissipation. a Q-factor vs polymer anchor width for different beam lengths and polymer thickness of 1 μm; error bars were calculated with the semi-range method by performing two sets of measurements on one device for each geometry. b Schematic of the structure with variable width.

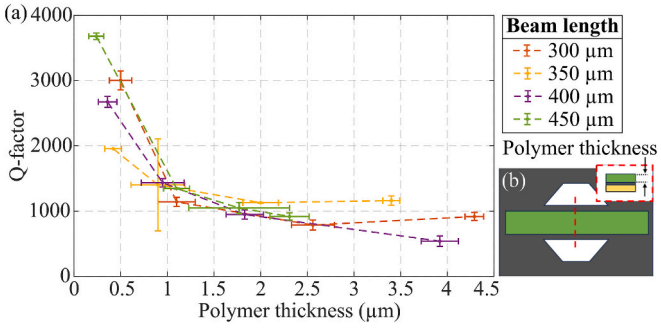

Fig. 4. Experimental study of the polymer intrinsic dissipation. a Q-factor vs polymer thickness for different beam lengths; error bars were calculated with the semi-range method by performing two sets of measurements on three devices for each geometry. b Schematic of the structure with variable polymer thickness.

proportional to the mass of the printed layer and a significant decrease of Q. Fig. 2 shows the variation of the measured fundamental frequency and Q-factor for different beam lengths after printing 1 μm thick polymer layer. The origin of dissipation was studied by analyzing two different dissipation sources.

3.3.1. *Clamping dissipation*

The effects of the printed polymer on anchor dissipation were investigated by varying the anchor width of the IP-Dip layer for different beam lengths. The corresponding experimental results are presented in Fig. 3. The overall dissipation of the beam is dominated by the polymer layer, as evidenced by the two-order-of-magnitude reduction in the Q-factor upon printing of a 1 μm thick polymer layer. Therefore, if anchor losses through the polymer were the dominant dissipation mechanism, an increase in the polymer mass would result in a decrease in the Q-factor. However, the absence of such a trend in the experimental data suggests that anchor losses are not the principal source of polymer-induced dissipation.

3.3.2. *Intrinsic dissipation*

To study the intrinsic dissipation in the polymer, the volume of IP-Dip was varied by changing its thickness. The measured Q-factors are shown in Fig. 4, displaying a decrease of Q with increasing IP-Dip thickness. Dissipation in the polymer is due to the extension and compression of the layer, which causes internal friction generated by the relative movements of monomer chains [10]. The greater the polymer volume, the greater the energy dissipated. Error bars of some experimental data show spread attributed to the large variability of the polymer thickness.

3.4. *Model for intrinsic dissipation in IP-Dip layer*

A viscous model was defined to describe the effects of the 3D-printed polymer on the dynamic response of the beam; in particular, the resonant frequency and the quality factor. The model is an extension of the viscous model proposed by Sader to define the dissipation and added mass in beams immersed in liquid [11,12]. In Sader's work, the interaction between the resonating beam and the surrounding liquid is characterized by two functions that defines the load exerted by the fluid, in terms of added mass and viscous damping. Similarly, in our structure, the polymer layer affects the overall inertia and damping. In addition, the viscoelastic nature polymer also has an elastic effect, described by the real component of the Young's modulus of the polymer, and results in an increase of the overall stiffness of the resonator. However, the elastic effect in our beam is outweighed by the inertia caused by the added mass of the polymer. In fact, the Young's modulus of IP-Dip is much smaller than that of SiN_x and the overall stiffness is largely unaffected, as proved by the reduction in resonant frequency when polymer is added to SiN_x beams. The uniform polymer layer can thus be treated as a distributed load that acts as an inertial-dissipative load and can be modeled using a

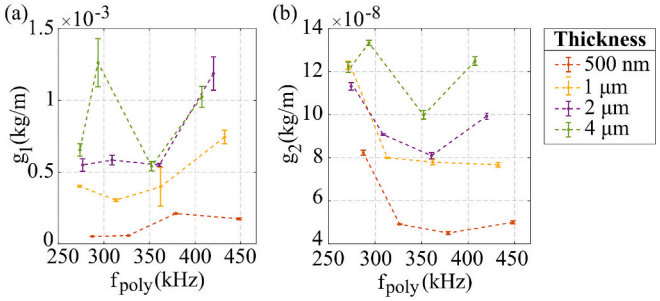

Fig. 5. Experimental values of the resonator geometry-dependent constants. a Distributed polymer damping g_1 and b distributed polymer equivalent added mass g_2 vs resonant frequency of SiN_x metal coated beams with 3-D printed layer for different polymer thickness.

distributed damping (g_1) and a distributed added mass (g_2), both per unit length [13]. The resonant frequency f_{poly} and the Q-factor Q_{visc} associated with polymer viscous losses can be obtained from the parameters g_1 and g_2:

$$f_{poly} = \frac{f_0}{\sqrt{1 + g_2/\mu}} \tag{2}$$

$$Q_{visc} = 2\pi f_0 \frac{\sqrt{1 + g_2/\mu}}{\sqrt{g_1/\mu}} \tag{3}$$

where μ is the longitudinal mass density of the beam and f_0 is the natural frequency of the metal-coated SiN_x beam without polymer in vacuum.

In our structure, g_1 and g_2 are geometry-dependent factors related to the properties of the solid layer. In particular, g_2 is a function of the mass density of the polymer, and g_1 is a function of its imaginary Young's modulus, responsible for the viscous dissipation. The experimental values calculated for g_1 and g_2 are reported in Fig. 5. The extracted parameters exhibit a dependence on the polymer thickness, with increasing thickness resulting in higher added mass and damping. No significant frequency dependence is observed in the data within the frequency range analyzed. In fact, a frequency dependence is expected due to the frequency-dependent Young's modulus.

4. Conclusion

Quality factors of double-clamped microbeams with an IP-Dip layer were measured and their dissipation mechanisms were investigated. After excluding polymer dissipation at the anchors as a dominant damping mechanism, it has been proven that dissipation is primarily due to intrinsic damping within the polymer layer. The intrinsic damping and frequency shift due to the IP-Dip layer were expressed using a viscous model. The model allows for the experimental extraction of effective mass and damping parameters to analyze the polymer contribution to energy dissipation in polymer-coated resonators. This approach is particularly relevant in applications involving soft polymer coatings, such as micro- and nanomechanical sensors for mass detection and chemical sensing [14–17], and dynamic mechanical analysis of thin films [18,19].

Declaration of competing interest

The authors declare that they have no known competing financial interests or personal relationships that could have appeared to influence the work reported in this paper.

Acknowledgements

The authors thank Prof. Carlo Ricciardi of Politecnico di Torino, Italy for the cooperation and administrative coordination of the master thesis work of Lucia Crocetto at the Delft University of Technology, The Netherlands. The technical support from the department of Precision and Microsystems Engineering, department of Microelectronics, and Else Kooi Laboratory cleanroom of the Delft University of Technology is highly appreciated.

Data availability

Data will be made available on request.

References

[1] F. Battiston, J.-P. Ramseyer, H. Lang, M. Baller, C. Gerber, J. Gimzewski, E. Meyer, H.-J. Èntherodt, A chemical sensor based on a microfabricated cantilever array with simultaneous resonance-frequency and bending readout, Sensors Actuators B Chem. 77 (2001), https://doi.org/10.1016/S0925-4005(01)00683-9.
[2] P. Belardinelli, L. Hauzer, M. Šiškins, M. Ghatkesar, F. Alijani, Modal analysis for density and anisotropic elasticity identification of adsorbates on microcantilevers, Appl. Phys. Lett. 113 (2018) 143102, https://doi.org/10.1063/1.5047279.
[3] G. Göring, P.-I. Dietrich, M. Blaicher, S. Sharma, J. Korvink, T. Schimmel, C. Koos, H. Hölscher, Tailored probes for atomic force microscopy fabricated by two-photon polymerization, Appl. Phys. Lett. 109 (2016), https://doi.org/10.1063/1.4960386.
[4] J. Winter, T. Manzaneque, M. Ghatkesar, Damping of 3d-printed polymer microbeam resonators, J. Micromech. Microeng. 34 (2023), https://doi.org/10.1088/1361-6439/ad08ef.
[5] K. Yasumura, T. Stowe, E. Chow, T. Pfafman, T. Kenny, B. Stipe, D. Rugar, Quality factor in micron- and submicron-thick cantilevers, J. Microelectromech. Syst. 9 (2000), https://doi.org/10.1109/84.825786.
[6] Y. Liu, J. Campbell, O. Stein, L.J. Jiang, J. Hund, Y. Lu, Deformation behavior of foam laser targets fabricated by two-photon polymerization, Nanomaterials 8 (2018) 498, https://doi.org/10.3390/nano8070498.
[7] S. Schmid, L.G. Villanueva, M.L. Roukes, Fundamentals of nanomechanical resonators, springer international publishing, Cham (2016), https://doi.org/10.1007/978-3-319-28691-4_2.
[8] G.G. Stoney, The tension of metallic films deposited by electrolysis, Proc. R. Soc. Lond. 82 (1909) 172–175, https://doi.org/10.1098/rspa.1909.0021.
[9] R. Sandberg, K. Molhave, A. Boisen, W. Svendsen, Effect of gold coating on the q-factor of a resonant cantilever, J. Micromech. Microeng. 15 (2005), https://doi.org/10.1088/0960-1317/15/12/006.
[10] J. Deutsch, Internal dissipation of a polymer, Phys. Rev. E Stat. Nonlinear Soft Matter Phys. 81 (2010) 061804, https://doi.org/10.1103/PHYSREVE.81.061804.
[11] J. Chon, P. Mulvaney, J. Sader, Experimental validation of theoretical models for the frequency response of atomic force microscope cantilever beams immersed in fluids, J. Appl. Phys. 87 (2000), https://doi.org/10.1063/1.372455.
[12] J. Sader, Frequency response of cantilever beams immersed in viscous fluids with applications to the atomic force microscope, J. Appl. Phys. 84 (1998), https://doi.org/10.1063/1.368002.
[13] I. Dufour, E. Lemaire, B. Caillard, H. Debéda, C. Lucat, S. Heinrich, F. Josse, O. Brand, Effect of hydrodynamic force on microcantilever vibrations: applications to liquid-phase chemical sensing, sensors and actuators B, Chemical 192 (2014) 664–672, https://doi.org/10.1016/j.snb.2013.10.106.
[14] L. Crocetto, Development of Hybrid Suspended Microchannel Resonators for Mass Sensing in Liquid, Master's thesis, Politecnico di Torino, 2023, http://webthesis.biblio.polito.it/29443/.
[15] S. Singamaneni, M.C. LeMieux, H.P. Lang, C. Gerber, Y. Lam, S. Zauscher, P. G. Datskos, N.V. Lavrik, H. Jiang, R.R. Naik, T.J. Bunning, V.V. Tsukruk, Bimaterial microcantilevers as a hybrid sensing platform, Adv. Mater. 20 (4) (2008) 653–680, https://doi.org/10.1002/adma.200701667.
[16] M. Possas-Abreu, F. Ghassemi, L. Rousseau, E. Scorsone, E. Descours, G. Lissorgues, Development of diamond and silicon mems sensor arrays with integrated readout for vapor detection, Sensors 17 (6) (2017), https://doi.org/10.3390/s17061163.
[17] Y. Dong, W. Gao, Q. Zhou, Y. Zheng, Z. You, Characterization of the gas sensors based on polymer-coated resonant microcantilevers for the detection of volatile organic compounds, Anal. Chim. Acta 671 (1) (2010) 85–91, https://doi.org/10.1016/j.aca.2010.05.007.
[18] L.Q. Nguyen, P.E. Larsen, T. Larsen, S.B. Goswami, L.G. Villanueva, A. Boisen, S. S. Keller, Pyrolytic carbon resonators for micromechanical thermal analysis, Microsyst. Nanoeng. (2019), https://doi.org/10.1038/s41378-019-0094-x.
[19] T. Liu, S. Pihan, M. Roth, M. Retsch, U. Jonas, J. Gutmann, K. Koynov, H.-J. Butt, R. Berger, Frequency response of polymer films made from a precursor colloidal monolayer on a nanomechanical cantilever, Macromolecules 45 (2012) 862–871, https://doi.org/10.1021/ma202396h.